Combined SECM-fluorescence microscopy using a water-soluble electrofluorochromic dye as the redox mediator

L. Guerret-Legras, J.F. F Audibert, I M Gonzalez Ojeda, G.V. Dubacheva, F. Miomandre

Combined SECM-fluorescence microscopy using a water-soluble electrofluorochromic dye as the redox mediator

L. Guerret-Legras, J.F. Audibert, I.M. Gonzalez Ojeda, G.V. Dubacheva and F. Miomandre*

PPSM – CNRS – ENS Paris-Saclay, 61 Avenue Président Wilson, 94235 Cachan, France

Abstract

A combined experiment of fluorescence and electrochemical microscopies was performed to highlight the possibility of using a unique water-soluble molecule as the redox mediator and fluorescence reporter. Resorufin was selected as it owns a highly luminescent redox state which can be easily converted into a non-emissive one by reduction at moderately negative potentials. In the feedback mode of Scanning Electrochemical Microscopy (SECM), it is shown that the fluorescence modulation amplitude is sensitive to the nature of the substrate as well as to the tip-substrate distance and can thus be utilized to record optical approach curves. Changing the polarization of the ITO substrate enables to move from positive to negative feedback and the fluorescence modulation amplitude is also sensitive to this change. Substrate generation-tip collection mode was also investigated showing that fluorescence intensity can be used to detect at the tip the species produced at the substrate with a higher accuracy than the electrochemical current.

Keywords: SECM, fluorescence microscopy, resorufin, electrofluorochromism

1. Introduction

The combination of optical techniques with electrochemistry has known a dramatic development in the two past decades especially at the microscopic level[1]. Optics in general allows imaging and investigating phenomena at the single event level, where its intrinsically high signal to noise ratio compared to electronics becomes a great advantage. Besides, the optical signal can be modulated at high frequency allowing detection of short-lived species. Several optical techniques have been recently coupled to electrochemistry among which holography[2], surface plasmon resonance (SPR)[3] and of course fluorescence, which displays both bright imaging and high sensitivity features. Fluorescence microscopy either in epifluorescence, confocal[4], or TIRF[5] configuration is a well-known imaging technique widely used to investigate chemical or biochemical events. Its coupling with electrochemistry is now well established and documented[6, 7]. It was demonstrated to be an efficient way for reporting redox reactions when one species is emissive in one redox state either when directly involved [8, 9] or when coupled to it through bipolar electrodes[10]. On the other hand, electrochemical microscopy known as SECM[11, 12] has also become popular for various applications like surface analysis, etching, that is surface writing and readout processes. It has become more recently a tool of choice for nanoelectrochemistry due to the improvement in the design of nanoelectrodes[13]. Combining optical techniques with SECM has been a topic of interest as well, for instance using Surface Plasmon Resonance

(SPR)[14], ECL[15] or fluorescence to image processes that were triggered by an electrochemical signal[16, 17] or even simply using a tip incorporating an optical fiber for dual electrochemical and optical scanning[18, 19]. More recently, SECM and fluorescence microscopy were successfully coupled to investigate biochemical events like detection of ROS in human cells[20] or ion permeation through nuclear pore complex[21], highlighting the power of such hyphenated techniques to investigate complex phenomena. It is worth mentioning that in most cases the electrochemical and fluorescence responses are considered independently as they come from different probes. However there are examples where using a single moiety as the fluorescent and redox reporter are especially useful[22]. On our side we recently published the use of a such a fluorescent and redox active (that is electrofluorochromic, EF) species in a combined in situ SECM and fluorescence microscopy experiment[23]. However, this example based on a tetrazine derivative was restricted to organic solvents due to its solubility and possible reactivity issues in water. In the present paper, we wish to extend the concept to aqueous solutions, which is especially suited when dealing with biological issues. We selected resorufin as the EF dye since, beyond its use as a probe in several biological events[24-27], it was also recently reported in fluorescence microscopy coupled to electrochemistry experiments[28]. Resorufin (RF) is highly fluorescent with an emission maximum at 592 nm in its anionic form and becomes non-fluorescent in its reduced protonated-anionic dihydroresorufin (DH) form (see scheme 1). Thus the electrode potential can be used to reversibly switch RF fluorescence in a similar way as already reported for tetrazines[29], but with the advantage of being usable in water. Moreover, the properties of the ITO-electrolyte interface may dramatically change from organic solvent to water[30]. This is also a reason why investigating the electrochemically monitored fluorescence switch at the ITO surface in aqueous solution is definitely of interest in comparison with previous reports in acetonitrile. In the present paper, we will demonstrate that RF can behave both as a redox mediator and fluorescent reporter in a combined SECM-fluorescence microscopy experiment, using either feedback or substrate generation- tip collection mode.

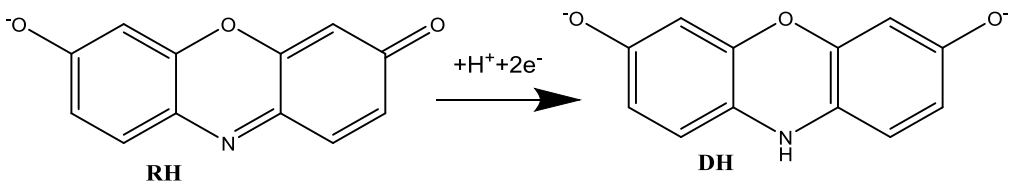

Scheme 1: Reduction reaction between emitting resorufin (RH) and non-emitting dihydroresorufin (DH)

2. Experimental

Chemicals. Resorufin (Sigma Aldrich, dye content 95%) was investigated at the concentration of 1.1 mM in a 0.05 M carbonate buffer solution (25 mM $NaHCO_3$, 25 mM Na_2CO_3, pH 10) prepared with ultrapure water (Milli-Q system, Millipore). Before each experiment, argon bubbling was used to remove dissolved oxygen from this solution. The argon flow was then maintained at low rate above the solution during all the acquisitions.

Resorufin, sodium bicarbonate (VWR chemicals) and sodium carbonate (VWR chemicals) were used without further purification.

Electrochemical measurements. The set up combining a Scanning Electrochemical Chemical Microscope and an inverse epifluorescence microscope was the same as described in ref.[23]. All electrochemical and SECM measurements were performed at room temperature using a homemade three-electrode spectroelectrochemical cell on top of an inverted optical microscope (see below). A platinum wire and a Ag/AgCl wire were used as a counter and reference electrode respectively. Glass coverslips (purchased from VWR, 1 mm thickness) and ITO (purchased from Solems, 25-35 ohm.□, 80 nm thickness) were employed as the substrates and working electrode in the case of ITO. A UME made of a 20 µm diameter platinum disk (purchased from Ametek) was used as the tip and second working electrode and positioned above the substrate thanks to a mechanic arm connected to a piezo positioner (VersaSCAN motion controller) which enables to control the tip position under VersaSCAN Software. Cyclic voltammetries were carried out with Versa Studio software at 10 mV/s with an intensity filter (1 Hz) for the tip. All approach curves were obtained with the microelectrode polarized at -0.75V vs Ag|AgCl and moving by 5 µm steps at the speed of 10 µm/s. The simultaneous control of the UME and substrate potentials is carried out thanks to a bipotentiostat (VersaSTAT 3F setting in floating mode for the tip and VersaSTAT 4 for the substrate, Ametek) under VersaStudio software.

Optical measurements. Optical measurements were performed on an inverted microscope (Ti Eclipse Nikon) with a 40X (X1.5) NA 0.75 objective in a wide field epi-illumination. Resorufin was excited by the association of a Hg lamp (Intensilight Nikon) with a band pass excitation filter (BP562 nm/40 nm) and FF593-Di03 dichroic (593 nm). Emitted light is collected through a long pass emission filter (LP 593 nm). Acquisition time-lapses are carried out using a CCD Pixel Fly camera from PCO at 14.2 images/s under the µManager open source software. Fluorescence intensity over time is reported as the mean intensity inside a square region of interest (ROI) (unless specified otherwise 94 x 94 pixels, red square in Figure 1A) of the total image centered on the tip. Emission spectra are recorded with an Ocean Optics spectrometer coupled to the microscope with a UV-VIS (400 µm diameter) optical fiber plus collimator placed in an intermediate image plane, with a 60 µm MFD (Mode Field Diameter) in the sample plane centered around the tip. Spectra are corrected from optical chain sensitivity and background and recorded with an interval time of 25 ms, 4.06 spectra/s.

Acquisition procedure. The acquisition procedure is the same as described in ref.[23]. First the contact of the tip with the substrate was determined optically (position z=0) and centered in the camera field; then a 500 µm depth approach curve was recorded. Afterwards the tip was positioned close to the substrate at a distance spotted on the approach curve and raised step by step (typically 5 µm steps). At each tip/substrate distance, the same spectroelectrochemical measurement was carried out. In the generation-collection mode, the substrate is allowed to go back to open circuit for at least 2 minutes between each tip position.

3. Results and discussion

The electrochemical modulation of the RF fluorescence intensity was recorded and analyzed in the various SECM modes: negative feedback, positive feedback and generation-collection. In parallel fluorescence images are recorded within the ROI around the SECM tip (fig. 1A) and the various images can be seen respectively in fig. 1B for insulating substrate and fig. 1C for conductive substrate.

3.1 Negative feedback

In negative feedback, only the tip can be used to control the redox state of the fluorophore and thus monitor the fluorescence intensity at the local scale. When the tip potential is stepped to -0.75 V, a potential negative enough to reduce RF in non-fluorescent DH, the fluorescence intensity is expected to drop. Figure 1B shows the fluorescence images recorded when applying various potential values at the tip. In absence of polarization (o.c. potential), the ROI centered on the tip shows a bright spot which becomes fully dark when the tip is polarized at -0.75 V. Fluorescence is restored when the tip potential is set back at 0 V and different contrasts can be seen depending on the time at which the image is recorded even at the same tip potential (compare b-c and d-e in fig. 1B).

In a second experiment, fluorescence intensity is measured vs. tip-substrate distance. Figure 2A shows the classical electrochemical approach curve, that is based on the tip current related to RF reduction. As the tip approaches the substrate, the current drops within the distance range from 0 to ca. 40 µm, as expected for negative feedback curves. Moreover, the current vs. tip position curve has been fitted with the expression of Lefrou et al.[31] showing a good agreement despite slightly lower experimental currents when the tip remains far from the substrate, possibly because of the overestimation of the normalization current due to residual oxygen (see fig. SI-1). Then the fluorescence intensity vs. time is measured (fig. 2B) for the following conditions: at each position of the tip, the potential is stepped from o.c. to 0 V and then to -0.75 V for 30 s before being set back to 0 V (see figure 2C). The corresponding variation of fluorescence intensity is shown in figure 2B and is called chronofluorogram: during the period when a negative potential is applied, the fluorescence intensity drops and goes back to its initial value when the potential is set back to 0 V. Finally, the amplitude of the modulation, defined as I.M. = $(I_{max}-I_{min})/I_{max}$ is plotted against tip position in figure 2A. The corresponding plot is overlaid with the electrochemical approach curve. It is clear that I.M. is sensitive to the distance between tip and substrate, since it starts to increase from ca. 60 µm. When the tip approaches closer to the substrate, the modulation amplitude increases, whereas the electrochemical reaction becomes less efficient (negative feedback). This is mainly due to the fact that the tip penetrates more deeply in the field of the objective. Thus, in the negative feedback mode, an equivalent approach curve can be obtained based on the optical signal, but with an increasing output value as the tip gets closer to the substrate, contrarily to the electrochemical current that fades away. Interestingly the distance at which the modulation amplitude starts to be sensitive to the substrate is significantly lower for RF than for tetrazine (Tz)[23]. This is probably due to the difference in the absorption coefficients (ε_{RF}(570 nm) = 51000$\pm$ 2800 $M^{-1}cm^{-1}$ vs. ε_{Tz}(520 nm) $\cong$ 500 $M^{-1}cm^{-1}$). When the tip moves away from the substrate, the first liquid layers are likely to absorb almost all the excitation light and molecules close to the tip are less excited. This effect is confirmed when looking at the calibration curve where I_{max} is plotted vs. the tip-substrate distance (figure SI-2). While the plot was linear on the whole

range of explored distance (500 µm) for Tz, here a curvature appears above ca. 80 µm. This linearity loss could be ascribed to a less amount of excitation received by the molecules far away from the substrate. To confirm this assumption, we investigated more diluted solutions and indeed lowering the concentration leads to a recovery of linearity on a larger distance range (see figure SI-2). A concentration of 0.11 mM gives a linear relationship (r^2 =0.99064) on the full considered working distances. Then, to understand if the fast I.M. drop when the tip-substrate distance increases (in comparison to Tz) might be related to the limited penetration depth of excitation, I.M. against the tip position at the three different concentrations are compared in figure SI-3. Despite a low-significant contribution of the concentration on the I.M. variation at ca. 40 µm, the overall trend of the three curves is very similar. This demonstrates that the penetration depth of excitation is not affecting the optical approach curve and so there is no problem in using EF probes even with high absorption coefficient like RF.

At first sight, the shape of the I.M. vs tip position graph (fig. 2A) looks similar to the one obtained with tetrazine[23], with a maximum close to 0.5 (0.65 for Tz), except the decrease at very short tip-substrate distances, which is hardly visible with RF compared to Tz. In that sense, RF behaves more closely to the model which does not predict any decrease at the shortest distances[23]. As there is no difference between the refractive indexes of water and acetonitrile, an optical effect based on refraction should not be involved. It is more likely that this is related to a more focused excitation, which was confirmed by using a laser source instead of the white lamp.

Finally, emission spectra were collected and displayed in figure 3A. The emission spectra present a maximum near 600 nm as expected for RF in aqueous solution. These graphs highlight the fact that the emission spectra remain identical in shape over time. The emission spectra can also be used instead of the intensity measured with the camera to record chronofluorograms (figure 3B) similar to those of figure 2B. Nevertheless, the modulation amplitude seems to be relatively low. To evaluate it more precisely, chronofluorograms have been measured for the different tip positions and the modulation amplitude derived. The result is reported in Figure 3C. It appears that the modulation amplitude is roughly two times lower for the intensity drawn from emission spectra than for the one calculated with intensities coming from the CCD camera. This can be explained by the fact that the spectrophotometer collects light in a fixed ROI around the tip which is nearly three times larger than the one delimited by the red square used with the CCD (see fig.1A). To compare, the normalized modulation amplitude calculated with intensities from CCD camera images have been repeated for various ROI. The results are also displayed in Figure 3C. It emphasizes the crucial role of the ROI on the modulation amplitude values: the smaller the ROI, the higher the normalized modulation amplitude maximum and this maximum is almost three times higher in the case of the orange ROI than in the case of the blue one. Moreover, the I.M. curve calculated from the blue ROI, which is supposed to be more or less the same as the one of the collection region from the spectrophotometer, matches rather well with curve coming from the emission spectra. So it seems reasonable to ascribe the lower sensitivity of the modulation amplitude with intensities extracted from emission spectra simply to a larger light collection area.

3.2 Positive feedback

In the positive feedback mode, both the tip and substrate might be polarized independently. We will first examine the case where the substrate (ITO) remains at open circuit potential. Figure 4 displays the results in a similar way as figure 2 for the negative feedback mode, namely electrochemical approach curve (figure 4A), fluorescence intensity modulation at various tip positions (figure 4B) for the same kind of potential signal (figure 4C). An approach curve based on the modulation amplitude I.M. is also shown, overlaid with the one using the electrochemical current (figure 4A). As in the previous case, fluorescence intensity can be switched off by the tip when this latter is polarized negatively and the fluorescence restored when the tip potential is set back at 0 V. The modulation amplitude is sensitive to the tip-substrate distance and becomes larger as the tip gets closer to the substrate. As already observed for tetrazine in acetonitrile[23], the maximum reached is significantly lower (0.2) for positive feedback than for negative feedback (0.5). This can be explained by the efficiency of the electrochemical reaction at the substrate, which regenerates the emissive form (see figures SI-4 and SI-5 for respectively CV and values of o.c. potentials on ITO) and thus decreases the difference between the 'on' and 'off' states for the same tip-substrate distance. As noticed for negative feedback, there is no drop in I.M. at very short distance, as it was observed with Tz in acetonitrile.

Another striking result is the relation between the optical approach curve based on the fluorescence intensity modulation amplitude (I.M.) and the electrochemical kinetics at the substrate, which was already reported in our previous study[23]. When ITO is polarized at -0.5 V, the behavior changes drastically since the regeneration of the emitting species (RF) on the substrate is not observed anymore. This results in a negative feedback which is demonstrated by the electrochemical approach curve (figure 5A) that is similar to the glass substrate (see also the evolution of electrochemical currents upon tip polarization in figure SI-5). This is also clearly evidenced on the 'optical' approach curve where the maximal amplitude is again close to 0.5 as it was for insulating substrate. A practical consequence is that the tip can be positioned at the closest distance from the substrate simply by looking for the position where the modulation amplitude is close to 0.5 for insulating substrate and 0.2 for conducting substrate. As the fluorescence drop occurs very quickly when the tip potential varies from open circuit to the appropriate value for switch off, the time required to get each point can be shortened to a few seconds.

Fluorescence images were also recorded to visualize how tip and substrate potentials can control the emitted light at short distance (see fig. 1C). Starting from open circuit for both (image a) corresponding to the 'on' state, it is possible to switch off the emitted light by applying a negative potential (-0.85 V, image b), then to switch on the light on the tip only by polarizing this latter at -0.4 V while maintaining the potential of the substrate at -0.85 V (image c) and finally switch off again the tip when its potential is set back at -0.85 V. In that case, a high contrast is observed between the tip and the surrounding area, allowing to image precisely what happens on the tip.

3.3 Substrate generation- tip collection (SG-TC)

The final configuration explored concerns the substrate generation-tip collection. This mode is usually employed to probe the reaction occurring at the substrate and has been widely used in the case of oxygen reduction reaction[32, 33]. In the present case, the ITO substrate is polarized at a negative potential (-0.85 V) to generate the non-emissive DH species (the potential is slightly more negative than when using the tip for that purpose because the electrochemical reaction is slower on ITO than on platinum, see figure SI-4). The tip is used as a collector by polarizing it at a potential allowing the reoxidation of DH into RF. Thus a fluorescence increase is expected to be the optical signal demonstrating the actual collection. Moreover the reaction at the tip can be used to map the composition of the diffusion layer of the substrate since this latter is much larger than the diffusion layer of the tip itself[34].

The results obtained in the SG-TC mode are shown in figure 6. Figure 6A confirms that the fluorescence intensity increases as soon as the tip is polarized at a potential where the DH produced at the substrate is reoxidized into RF. Concerning the electrochemical current (fig. 6B), it is nearly constant whatever the tip-substrate distance during the collection period; indeed, the diffusion layer of the substrate extends far beyond this distance. A quick estimation of it $(\pi Dt)^{1/2}$ using the diffusion coefficient of RF ($2x10^{-6}$ cm^2s^{-1})[28] leads to a value close to 100 µm for a 15 s polarization which is consistent with the assumption. As the tip diameter is larger than the variation of the tip position within the diffusion layer, the tip current is fairly constant. Thus the corresponding increase in fluorescence intensity during the collection period as the tip moves farther from the substrate is simply due to the enlargement of the collection area. This can be seen also when looking at the variation of the initial fluorescence intensity (before polarizing ITO, 0-5 s) with the distance, which reproduces the variation of figure SI-2. When the tip is close to the substrate, the fluorescence recorded drops very fast as soon as ITO becomes polarized negatively, while for larger distances, the fluorescence drop becomes less and less steep and is clearly dominated by diffusion processes. This can be evidenced when plotting the tip-substrate distance as of a function of the square root of the time corresponding to a given fluorescence intensity in the 5-20 s range with time (see fig. SI-6). A linear variation with a reasonably good fit is obtained showing that the fluorescence quenching is under diffusion control in that time interval.

The tip collection process shows a stable fluorescence intensity during the collection period, whose value is directly related to the tip-substrate distance. The optical collection efficiency can be assessed by calculating the fluorescence recovery ratio $I_{collect}/I_{max}$, where $I_{collect}$ is the fairly constant fluorescence intensity measured during the collection period. Figure 7 shows how this ratio varies with the tip-substrate distance. While the electrochemical current is fairly the same at distances within the diffusion layer of the substrate, the fluorescence collection ratio does change and increases as the tip is closer. Once again, the optical detection brings additional information on the tip-substrate distance in a range where electrochemistry become insensitive.

4. Conclusion

Combination of SECM with fluorescence microscopy can be performed using a unique water-soluble species as fluorophore and redox mediator. In all the SECM modes investigated (feedback and generation-collection), the modulation amplitude, that is the normalized difference between the on and off intensities is very sensitive to the tip-substrate distance on one hand and to the reaction likely to occur on the substrate on the other hand. This proof of concept opens new possibilities for exploring either active substrates like plasmonic ones or for investigating electrochemically induced phenomena with the fluorescence as the output at the local scale and in biological conditions. Besides fluorescence images, intensity and spectra that are recorded under electrochemical control with the present set-up, the use of a pulse excitation will enable fluorescence lifetimes to be measured and its variation with the electrode potential to be analyzed. This is the purpose of our ongoing experiments to obtain a full set of fluorescence data likely to be useful especially in conditions where electrochemistry would not be informative anymore.

Acknowledgments

CHARMMMAT Labex and Region Ile-de-France (C'Nano network) are acknowledged for financial support of the setup.

The University of Michigan, promotor of the program 'Optics in the city of lights' is acknowledged for funding the internship of I.M. Gonzalez Ojeda.

References

[1] Kanoufi F. Editorial: Innovative Methods in Electrochemistry. Seeing electrochemistry with new eyes. Current Opinion in Electrochemistry 2017;6:1-3.
[2] Brasiliense V, Berto P, Combellas C, Tessier G, Kanoufi F. Electrochemistry of Single Nanodomains Revealed by Three-Dimensional Holographic Microscopy. Acc. Chem. Res. 2016;49:2049-57.
[3] Wang C, Sun L, Weber SG. Simultaneous optical fiber surface plasmon resonance (SPR) and electrochemistry sensing. Abstracts of Papers of the American Chemical Society 1997;213:236-ANYL.
[4] Shuman H, Murray JM, Dilullo C. CONFOCAL MICROSCOPY - AN OVERVIEW. Biotechniques 1989;7:154-&.
[5] Trache A, Meininger GA. Total internal reflection fluorescence (TIRF) microscopy. Curr. Protoc. Microbiol. 2008;Chapter 2:Unit 2A.2.1-2A.2.22.
[6] Miomandre F, Meallet-Renault R, Vachon JJ, Pansu RB, Audebert P. Fluorescence microscopy coupled to electrochemistry: a powerful tool for the controlled electrochemical switch of fluorescent moleculesw. Chem. Commun. 2008;16:1913.
[7] Bouffier L, Doneux T. Coupling electrochemistry with in situ fluorescence (confocal) microscopy. Current opinion in electrochemistry 2017;6:31-37.
[8] Miomandre F, Lepicier E, Munteanu S, Galangau O, Audibert JF, Meallet-Renault R, et al. Electrochemical Monitoring of the Fluorescence Emission of Tetrazine and Bodipy Dyes Using Total Internal Reflection Fluorescence Microscopy Coupled to Electrochemistry. ACS Appl. Mater. Int. 2011;3:690-96.
[9] de Poulpiquet A, Goudeau B, Garrigue P, Sojic N, Arbault S, Doneux T, et al. A snapshot of the electrochemical reaction layer by using 3 dimensionally resolved fluorescence mapping. Chem. Sci. 2018;9:6622-28.

[10] Oja SM, Guerrette JP, David MR, Zhang B. Fluorescence-Enabled Electrochemical Microscopy with Dihydroresorufin as a Fluorogenic Indicator. Anal. Chem. 2014;86:6040-48.
[11] Bard AJ, Mirkin MV, Unwin PR, Wipf DO. SCANNING ELECTROCHEMICAL MICROSCOPY .12. THEORY AND EXPERIMENT OF THE FEEDBACK MODE WITH FINITE HETEROGENEOUS ELECTRON-TRANSFER KINETICS AND ARBITRARY SUBSTRATE SIZE. J.Phys. Chem. 1992;96:1861-68.
[12] Liu HY, Fan FRF, Lin CW, Bard AJ. SCANNING ELECTROCHEMICAL AND TUNNELING ULTRAMICROELECTRODE MICROSCOPE FOR HIGH-RESOLUTION EXAMINATION OF ELECTRODE SURFACES IN SOLUTION. J.Am. Chem. Soc. 1986;108:3838-39.
[13] Kai T, Zoski CG, Bard AJ. Scanning electrochemical microscopy at the nanometer level. Chem. Commun. 2018;54:1934-47.
[14] Szunerits S, Knorr N, Calemczuk R, Livache T. Approach to writing and simultaneous reading of micropatterns: Combining surface plasmon resonance imaging with scanning electrochemical microscopy (SECM). Langmuir 2004;20:9236-41.
[15] Fan F-RF, Cliffel D, Bard AJ. Scanning Electrochemical Microscopy. 37. Light Emission by Electrogenerated Chemiluminescence at SECM Tips and Their Application to Scanning Optical Microscopy. Anal.Chem. 1998;70:2941-48.
[16] Boldt FM, Heinze J, Diez M, Petersen J, Borsch M. Real-time pH microscopy down to the molecular level by combined scanning electrochemical microscopy/single-molecule fluorescence spectroscopy. Anal. Chem. 2004;76:3473-81.
[17] Ku SY, Wong KT, Bard AJ. Surface patterning with fluorescent molecules using click chemistry directed by scanning electrochemical microscopy. J. Am. Chem. Soc. 2008;130:2392-93.
[18] Lee Y, Bard AJ. Fabrication and characterization of probes for combined scanning electrochemical/optical microscopy experiments. Anal. Chem. 2002;74:3626-33.
[19] Lee Y, Ding ZF, Bard AJ. Combined scanning electrochemical/optical microscopy with shear force and current feedback. Anal. Chem. 2002;74:3634-43.
[20] Salamifar SE, Lai RY. Use of Combined Scanning Electrochemical and Fluorescence Microscopy for Detection of Reactive Oxygen Species in Prostate Cancer Cells. Anal. Chem. 2013;85:9417-21.
[21] Kim J, Izadyar A, Shen M, Ishimatsu R, Amemiya S. Ion Permeability of the Nuclear Pore Complex and Ion-Induced Macromolecular Permeation as Studied by Scanning Electrochemical and Fluorescence Microscopy. Anal.Chem. 2014;86:2090-98.
[22] Liu XQ, Savy A, Maurin S, Grimaud L, Darchen F, Quinton D, et al. A Dual Functional Electroactive and Fluorescent Probe for Coupled Measurements of Vesicular Exocytosis with High Spatial and Temporal Resolution. Angew. Chem. Int. Ed. 2017;56:2366-70.
[23] Legras L, Audibert JF, Dubacheva GV, Miomandre F. Combined Scanning Electrochemical and Fluorescence Microscopies using a tetrazine as a single redox and luminescent (electrofluorochromic) probe. Chem. Sci. 2018; 9,5897-5905.
[24] Jenkins ATA, Dash HA, Boundy S, Halliwell CM, ffrench-Constant RH. Methoxy-resorufin ether as an electrochemically active biological probe for cytochrome P450 O-demethylation. Bioelectrochem.2006;68:67-71.
[25] Maeda H, Matsu-ura S, Senba T, Yamasaki S, Takai H, Yamauchi Y, et al. Resorufin as an electron acceptor in glucose oxidase-catalyzed oxidation of glucose. Chem. & Pharm. Bull. 2000;48:897-902.
[26] Qian Y, Lin J, Han L, Lin L, Zhu H. A resorufin-based colorimetric and fluorescent probe for live-cell monitoring of hydrazine. Biosensors & Bioelectronics 2014;58:282-86.
[27] Wang F, Li Y, Li W, Zhang Q, Chen J, Zhou H, et al. A facile method for detection of alkaline phosphatase activity based on the turn-on fluorescence of resorufin. Anal. Meth. 2014;6:6105-09.
[28] Doneux T, Bouffier L, Goudeau B, Arbault S. Coupling Electrochemistry with Fluorescence Confocal Microscopy To Investigate Electrochemical Reactivity: A Case Study with the Resazurin-Resorufin Fluorogenic Couple. Anal. Chem. 2016;88:6292-300.
[29] Kim Y, Kim E, Clavier G, Audebert P. New tetrazine-based fluoroelectrochromic window; modulation of the fluorescence through applied potential. Chem. Commun. 2006:3612-14.

[30] Memming R. Semiconductor electrochemistry 2nd edition. Weinheim: Wiley; 2015.
[31] Lefrou C, Cornut R. A unified new analytical approximation for negative feedback currents with a microdisk SECM tip. J.Electroanal. Chem. 2007;608:59-66.
[32] Sanchez-Sanchez CM, Rodiriguez-Lopez J, Bard AJ. Scanning electrochemical microscopy. 60. Quantitative calibration of the SECM substrate generation/tip collection mode and its use for the study of the oxygen reduction mechanism. Anal. Chem. 2008;80:3254-60.
[33] Johnson L, Walsh DA. Tip generation-substrate collection-tip collection mode scanning electrochemical microscopy of oxygen reduction electrocatalysts. J. Electroanal. Chem. 2012;682:45-52.
[34] Amatore C, Szunerits S, Thouin L. Mapping concentration profiles within the diffusion layer of an electrode Part II. Potentiometric measurements with an ultramicroelectrode. Electrochem.Commun. 2000;2:248-53.

Figure(s)

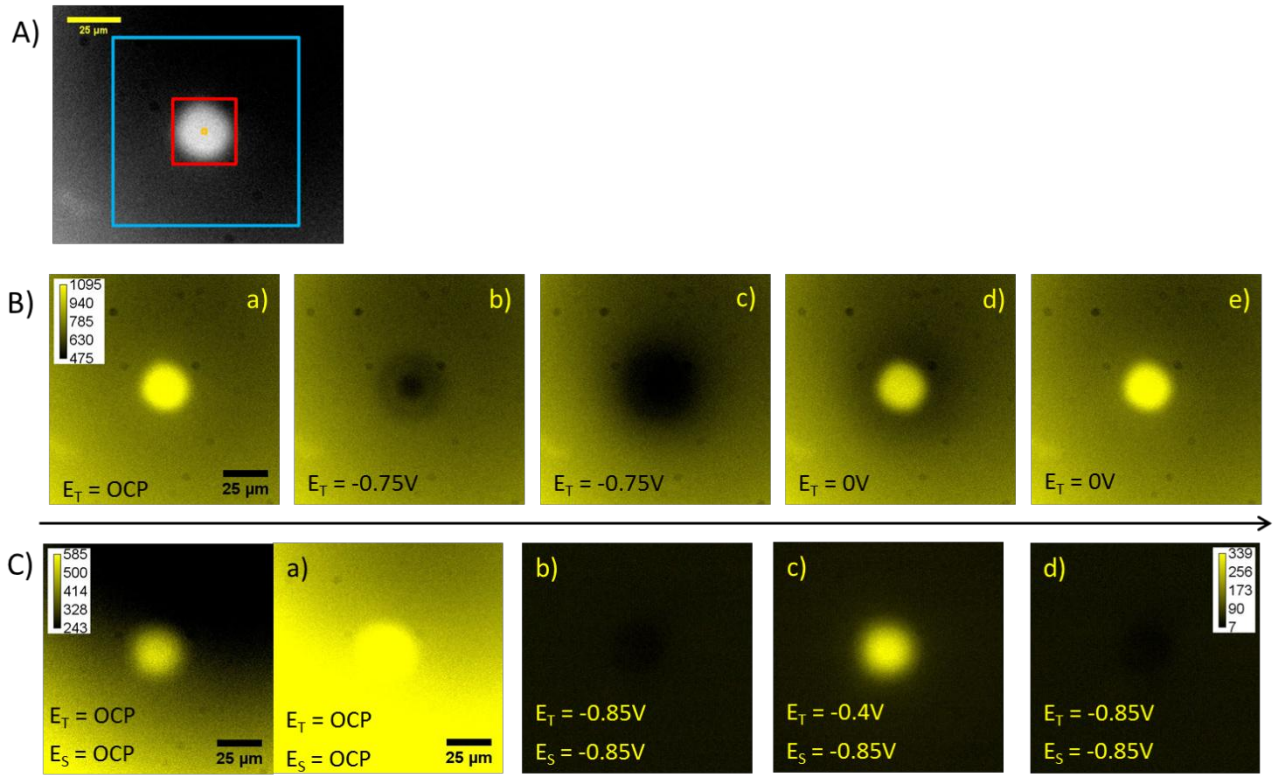

Figure 1: Region of interest (ROI) (A) and fluorescence images recorded with the CCD camera on glass substrate (B) or ITO substrate (C).

(A) ROI encompassing the tip used for data treament. The red one was systematically used. The blue one and the orange one correspond respectively to the large and small ROI in Fig.3B.

(B) Set of fluorescence images when the tip potential varies according to the following sequence: open circuit potential (ocp) (10 s), 0 V (10 s), -0.75V (30 s) and 0 V (20 s). Images (a), (b), (c), (d) and (e) are recorded respectively at t = 15, 23, 45, 52 and 68 s. Tip position: 5 µm.

(C) Set of fluorescence images when the substrate potential varies according to the sequence: ocp (5 s), -0.85 V (55 s) and the tip potential according to the sequence: ocp (10 s), -0.85 V (10 s), -0.4 V (30 s) and -0.85 V (20 s). Images (a), (b), (c) and (d) are recorded respectively at t = 4, 8, 45 and 65 s.Tip position < 5 µm. Images (a-e) in (B) are recorded with the same contrast settings. Images (a-d) in (C) are recorded with the same contrast settings. The first image in (C) is the same as (a) but with the same contrast setting as images in (B).

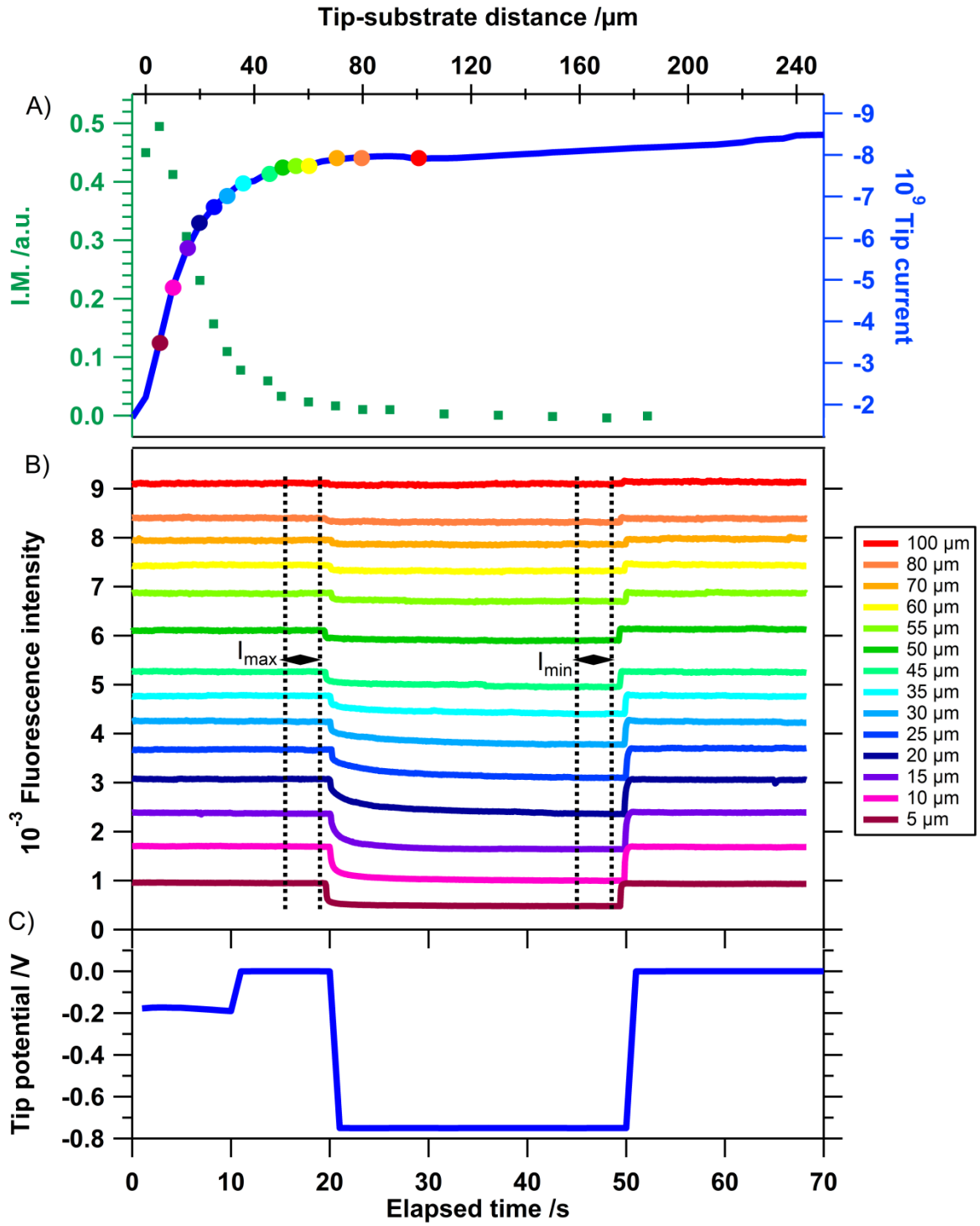

Figure 2 : Modulation of the fluorescence intensity with the tip potential vs. tip-substrate distance in the negative feedback mode (substrate: glass). (A) Approach curve (blue trace, right scale) at -0.75V and normalized fluorescence intensity modulation amplitude I.M.=(I_{max}-I_{min})/I_{max} (green squares, left scale) vs. tip position. See (B) for the definition of I_{max} and I_{min} and (C) for the corresponding potential values. (B) Fluorescence intensity vs. time (chronofluorogram) at various tip-substrate distances. (C) Potential vs. time signal applied at the tip at each position: ocp (10 s), 0 V (10 s), -0.75 V (30 s) and 0 V (20 s)

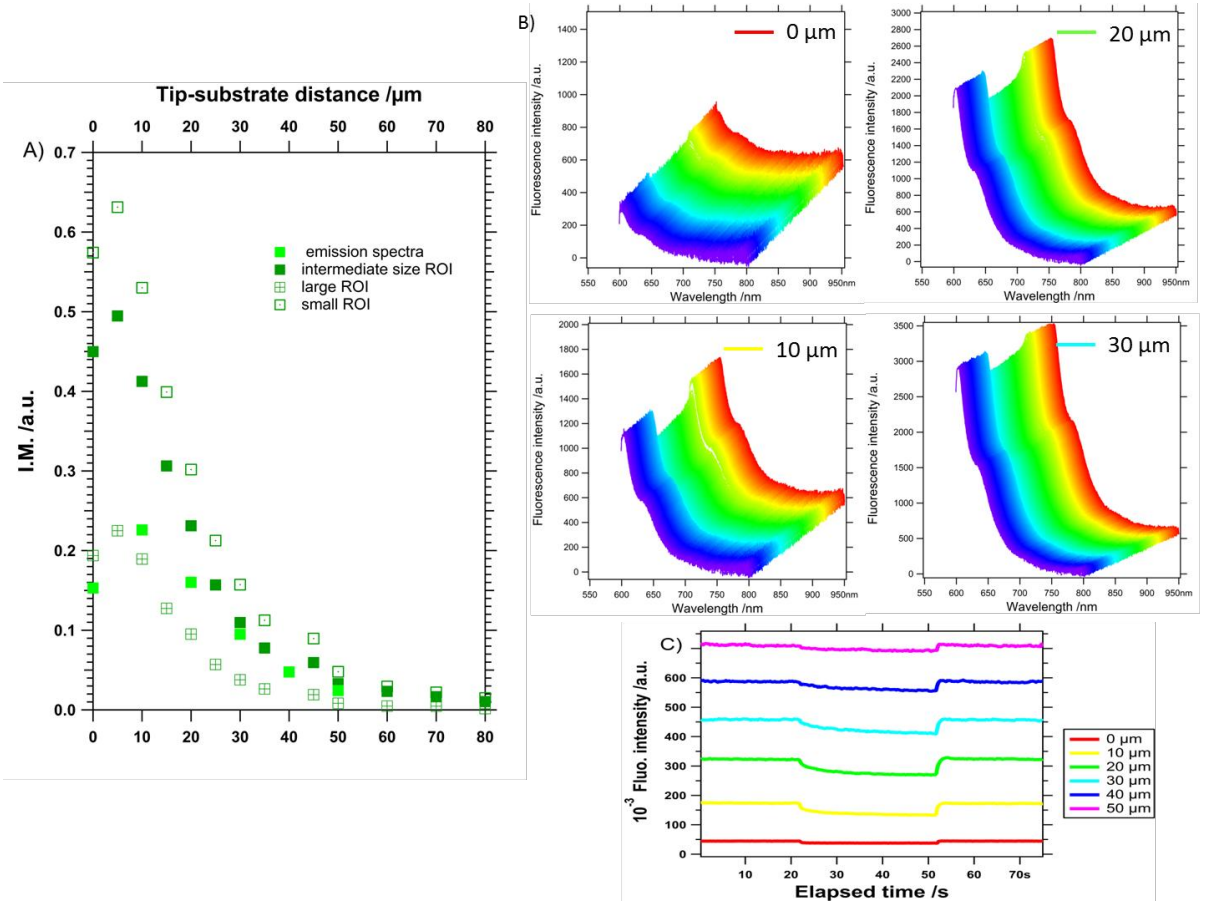

Figure 3: (A) Comparison between fluorescence intensity modulation amplitudes I.M.=(I_{max}-I_{min})/I_{max} extracted from integration of emission spectra (light green squares) with those calculated from chronofluorograms in Fig. 2B (dark green squares). For comparison similar curves obtained with the camera and different ROI sizes are overlaid (large and small ROI refer to the blue and orange ROI respectively in Fig.1A). (B) Emission spectra vs. time at different tip-substrate distances when the following potential signal is imposed to the tip: ocp (10 s), 0 V (10 s), -0.75 V (30 s) and 0 V (20 s) as in Fig.1C (substrate: glass). (C) Chronofluorograms at various tip-substrate distances obtained by integration of the corresponding emission spectra vs. time.

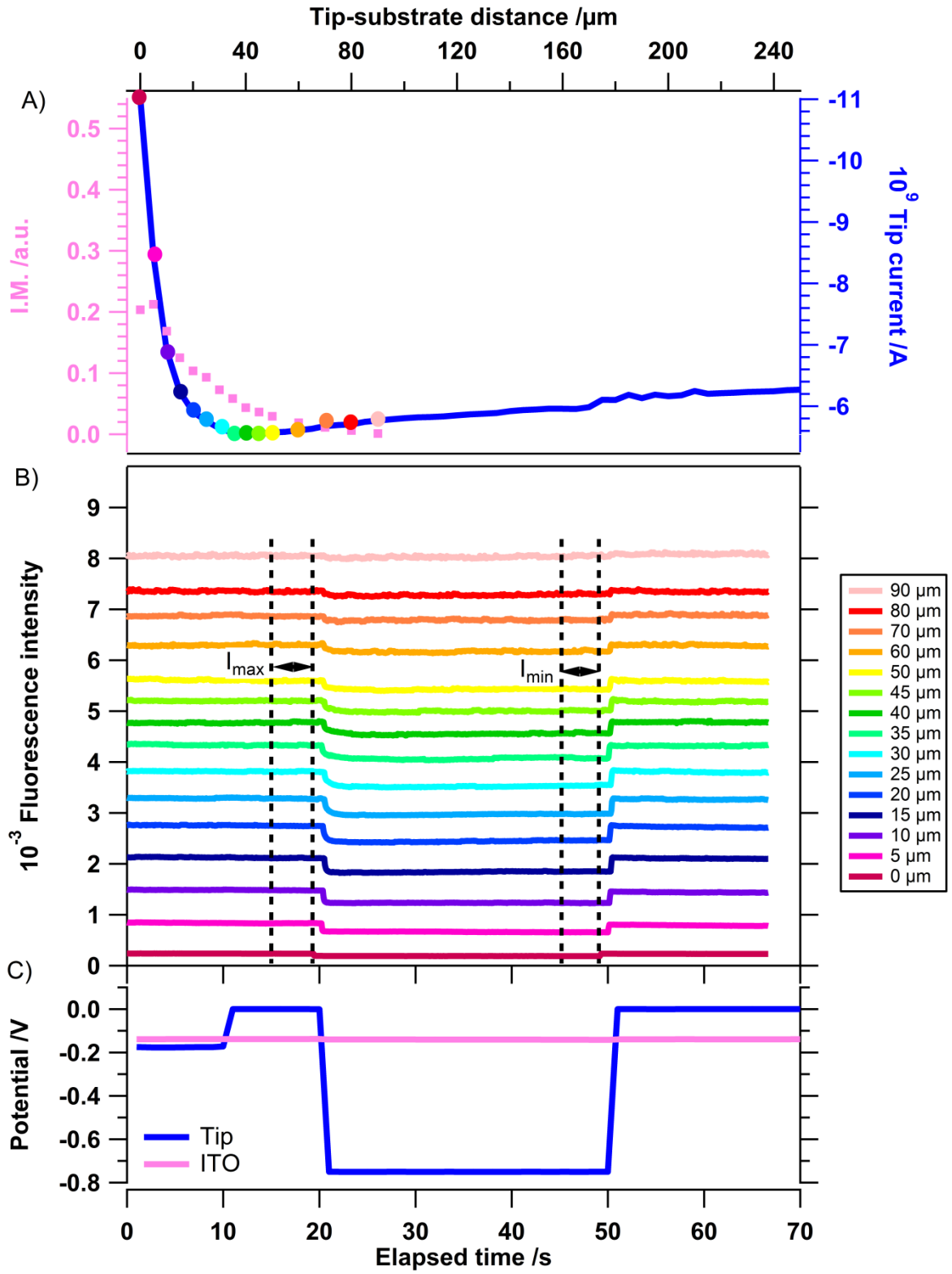

Figure 4: Modulation of the fluorescence intensity with the tip potential vs. tip-substrate distance in the positive feedback mode (substrate: ITO at open circuit potential). (A) Approach curve (blue trace, right scale) at -0.75 V and normalized fluorescence intensity modulation amplitude I.M.=(I_{max}-I_{min})/I_{max} (pink squares, left scale) vs. tip position. See (B) for the definition of I_{max} and I_{min} and (C) for the corresponding potential values. (B) Fluorescence intensity vs. time (chronofluorogram) at various tip-substrate distances. (C) Potential signal vs. time applied at ITO substrate and Pt tip.

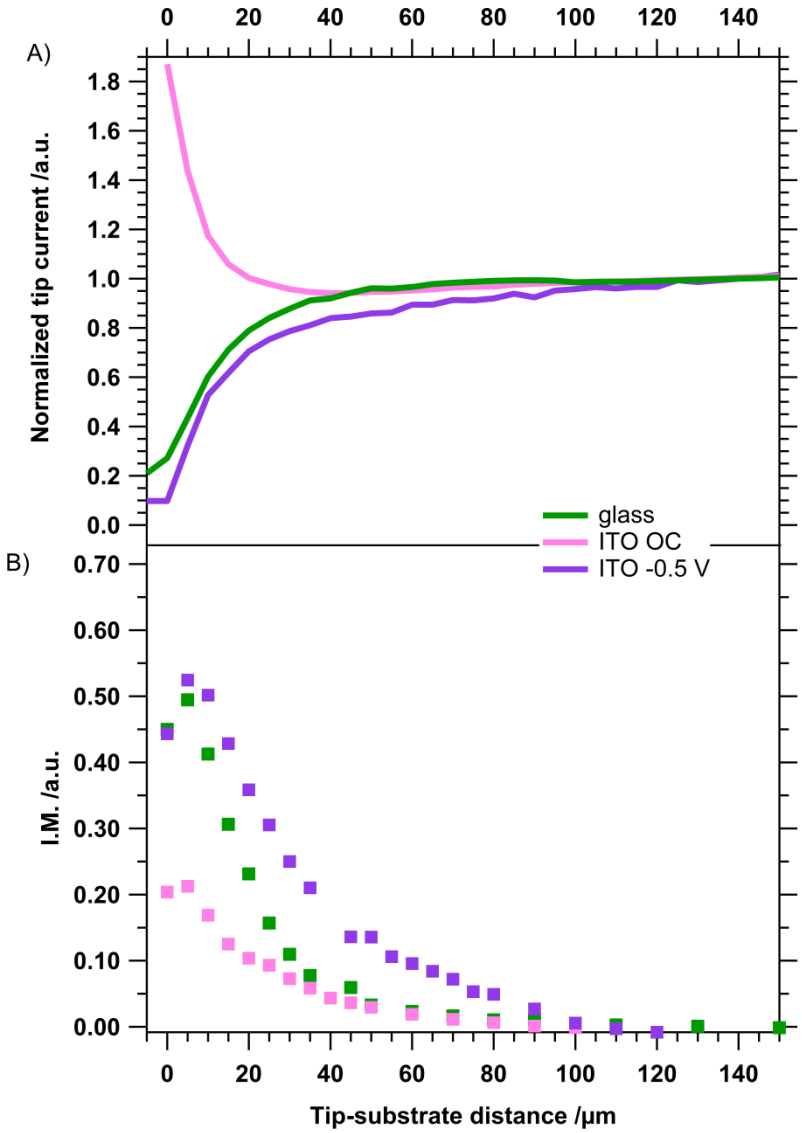

Figure 5 : (A) Normalized approach curves on various substrates. (B) Normalized modulation amplitude vs. tip-substrate distance for ITO polarized at -0.5V (purple), ITO at open circuit potential (green) and for glass (pink). The tip potential is stepped from 0 V to -0.75 V for all curves.

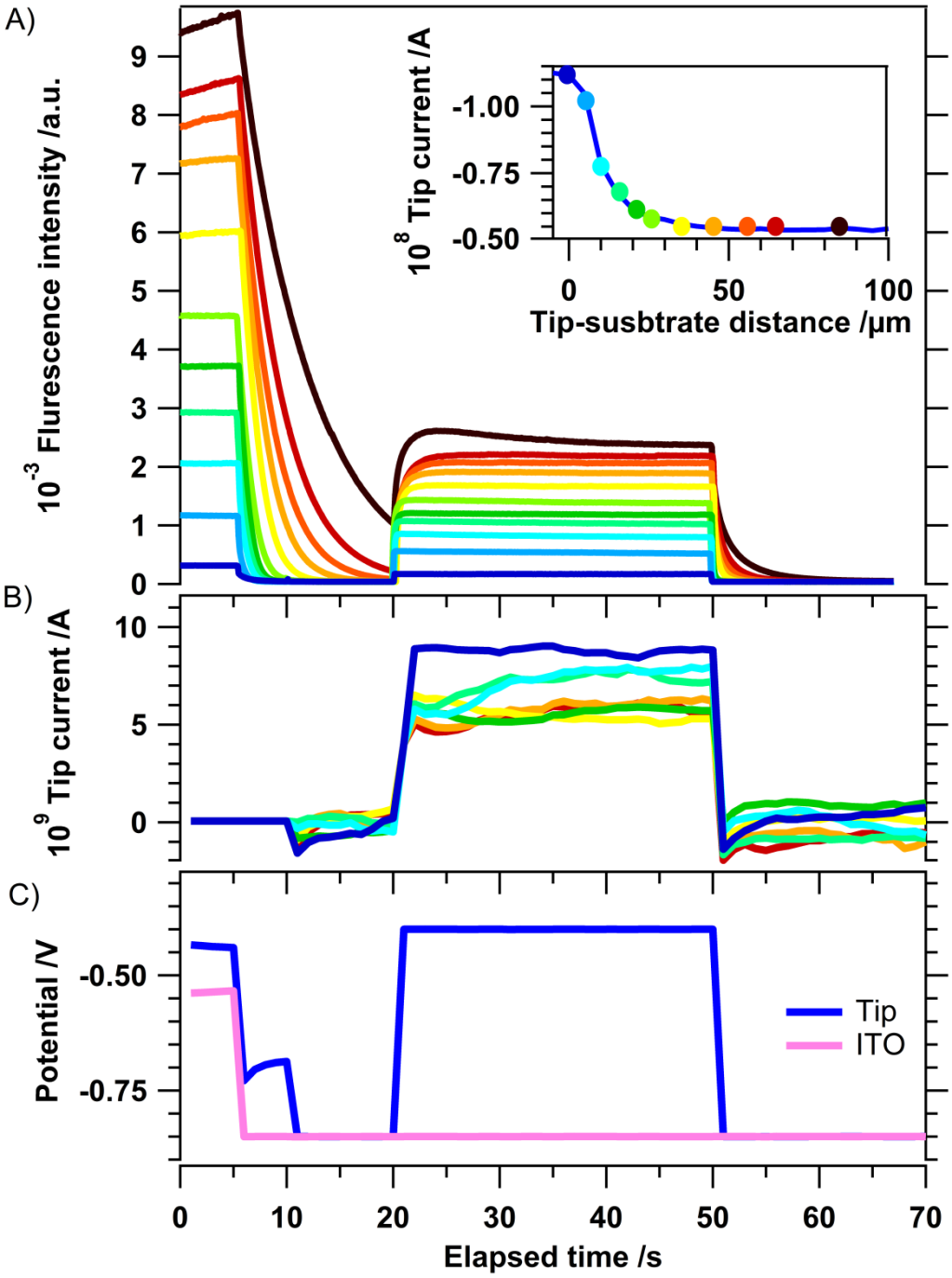

Figure 6: Substrate generation-tip collection (SG-TC) mode.

A) Fluorescence intensity vs. time for various tip-substrate distance values corresponding to the dots in the approach curve (see inset). B) Tip current vs. time for the same tip-substrate distance as in A). C) Tip and substrate potential signals used in the SG-TC experiment.

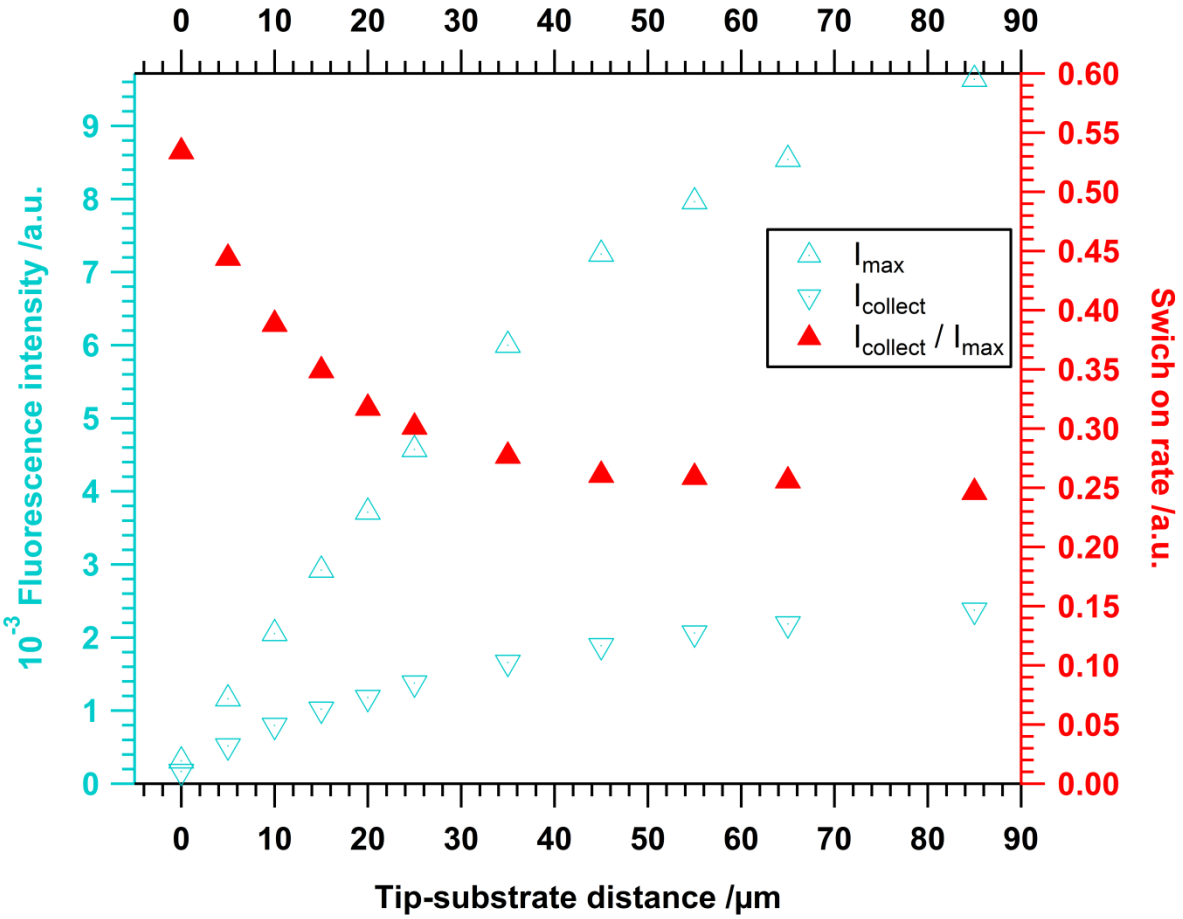

Figure 7: Fluorescence intensity recorded before ITO polarization (I_{max}) and during the collection period (20-50 s, see figure 6, $I_{collect}$) and collect ratio $I_{collect}/ I_{max}$ vs. tip-substrate distance.